Growth of Si/β-$FeSi_2$/Si double-heterostructures on Si(111) substrates by molecular-beam epitaxy and photoluminescence using time-resolved measurements

M. Takauji and N. Seki
Institute of Applied Physics, University of Tsukuba, Tsukuba, Ibaraki 305-8573, Japan

T. Suemasu[a] and F. Hasegawa
Institute of Applied Physics and Center for Tsukuba Advanced Research Alliance, University of Tsukuba, Tsukuba, Ibaraki 305-8573, Japan

M. Ichida
Department of Physics, Konan University, Kobe, Hyogo 658-8501, Japan

(Received 12 March 2004; accepted 27 May 2004)

Highly [110]/[101]-oriented semiconducting iron disilicide β-$FeSi_2$ continuous films were grown on Si(111) by molecular-beam epitaxy (MBE) using a β-$FeSi_2$ epitaxial template formed by reactive deposition epitaxy. The optimum MBE growth temperature was determined to be about 750 °C. At this temperature, the full width at half maximum β-$FeSi_2$(220)/(202) x-ray diffraction peak was at a minimum. Subsequent MBE overgrowth of an undoped Si layer was performed on the β-$FeSi_2$ at 500 °C, resulting in the Si/β-$FeSi_2$/Si double heterostructure. After annealing the wafers at 800 °C in Ar for 14 h, 1.55 μm photoluminescence (PL) was obtained at low temperatures. Time-resolved PL measurements elucidated that the luminescence originated from two sources, one with a short decay time ($\tau \sim 10$ ns) and the other with a long decay time ($\tau \sim 100$ ns). The short decay time was thought to be due to carrier recombination in β-$FeSi_2$, whereas the long decay time was due probably to a dislocation-related *D*1 line in Si. © *2004 American Institute of Physics*. [DOI: 10.1063/1.1774246]

I. INTRODUCTION

Semiconducting iron disilicide (β-$FeSi_2$) has been attracting much attention as a material for a Si-based light emitter with a wavelength ~1.5 μm, which would have applications to optical fiber communications.[1] The room temperature (RT) 1.6 μm electroluminescence (EL) has already been realized in *p*-Si/β-$FeSi_2$ particles /*n*-Si light-emitting diodes (LEDs) formed by ion beam synthesis (IBS) and by molecular-beam epitaxy (MBE) methods.[2–6] In an effort to make an efficient LED with a β-$FeSi_2$ active region, it is necessary to embed a β-$FeSi_2$ continuous film rather than particles in Si. Recently, Chu *et al.* reported EL from Si/β-$FeSi_2$/Si double heterostructures (DH), in which the β-$FeSi_2$ film was grown by a rf magnetron-sputtering technique, followed by chemical vapor deposition (CVD) of a Si overlayer.[7] The EL intensity was, however, comparable to that of Si at RT. This is the only report on EL from a Si/β-$FeSi_2$/Si DH to date. This is due to the difficulty in embedding a β-$FeSi_2$ continuous film in Si. In the case of IBS, implantation of high Fe doses is required in order to form a β-$FeSi_2$ continuous film in Si. Therefore, a tremendous number of defects are introduced. [8] Hence, lower doses of Fe are implanted in order to form β-$FeSi_2$ precipitates in LEDs produced by IBS.[2–4] In the case of reactive deposition epitaxy (RDE) (Fe deposition on hot Si) and molecular beam epitaxy [(MBE) (co-deposition of Fe and Si on hot Si)], a β-$FeSi_2$ epitaxial film grown on Si(001) exhibits a strong tendency to form islands.[9,10] In particular, the β-$FeSi_2$ epitaxial film easily aggregates into islands during high-temperature annealing.[11] High-temperature annealing is inevitable to improve the crystalline quality of β-$FeSi_2$ as well as its luminescence intensity. [12] Therefore, the β-$FeSi_2$ particles are used as an active region in LEDs grown by RDE and MBE.[5,6] However, there have been a few reports showing that smooth β-$FeSi_2$ films can be grown on Si(111) substrates even at high temperatures, in spite of the large lattice mismatch of approximately 5%.[13,14] The DH prepared by CVD described above was also formed on Si(111). However, there have been no reports on the formation of a Si/β-$FeSi_2$/Si DH on Si substrates by MBE.

The purpose of this investigation was to determine the optimum growth conditions for epitaxial growth of β-$FeSi_2$ films on Si(111) by MBE and a Si/β-$FeSi_2$/Si DH. The origin of 1.55 μm photoluminescence (PL) from the DH was investigated using time-resolved PL measurements.

II. EXPERIMENTAL METHOD

An ion-pumped MBE system equipped with electron gun evaporation sources for Si and Fe was used in this evaluation. A *p*-type floating zone Si(111) ($\rho = 1000-6000\ \Omega$ cm; $20 \times 20 \times 0.5$ mm^3) was used as the substrate. After cleaning the Si(111) substrate at 850 °C for 30 min in UHV, and confirming a well-developed 7×7 reflection high-energy electron diffraction, β-$FeSi_2$ films were grown by MBE as follows: A 20 nm-thick β-$FeSi_2$ epitaxial film was grown by RDE. This film was used as a template to control the crystal

[a]Electronic Mail: suemasu@bk.tsukuba.ac.jp

TABLE I. Sample preparation: Growth temperature and thickness of RDE- and MBE-grown β-$FeSi_2$ layers. Thickness of the Si overlayer is listed in parentheses. Annealing conditions are also specifield.

Sample	RDE/MBE	Si overlayer	Annealing
A	650°C(20 nm)/750°C(70 nm)	500°C(300 nm)	900°C/14 h
B	650°C(20 nm)/750°C(70 nm)	500°C(300 nm)	800°C/14 h
C	650°C(20 nm)/750°C(70 nm)	500°C(300 nm)	no
D	650°C(20 nm)/750°C(70 nm)	500°C(900 nm)	900°C/14 h
E	650°C(20 nm)/750°C(70 nm)	500°C(900 nm)	500°C/14 h
F	650°C(20 nm)/750°C(70 nm)	500°C(900 nm)	no

orientation of a β-$FeSi_2$ overlayer. The deposition rate of Fe was fixed at 0.6 nm/min, and the growth temperature was varied from 470 to 850°C in order to determine the optimum temperature. Then, Si and Fe were coevaporated on the β-$FeSi_2$ template at temperatures ranging from 550 to 850°C. The total thickness of the β-$FeSi_2$ film including the template was 90 nm. In order to control the stoichiometry of the MBE-grown films, the deposition rates of Fe and Si were controlled by using an electron impact emission spectroscopy (EIES) sensor for Fe and by maintaining constant input power of the electron-beam gun for Si, respectively. For the Si/β-$FeSi_2$/Si DH, a 20-nm-thick β-$FeSi_2$ template was grown by RDE at 650°C, followed by a 70-nm-thick β-$FeSi_2$ film grown by MBE at 750°C. These temperatures were optimized as detailed later. Next, undoped Si was grown on the β-$FeSi_2$ film at 500°C forming a DH. Finally, the wafers were annealed in an Ar atmosphere for 14 h at 800 or 900°C. Samples were prepared as summarized in Table I.

The crystal quality of the grown layers was characterized by x-ray diffraction (XRD), and the surface morphology and cross-sectional profile were observed by atomic force microscopy (AFM) and scanning electron microscopy (SEM). Steady-state PL was measured by the standard lock-in technique using a He-Cd laser (442 nm) and a liquid-nitrogen-cooled InP/InGaAs photomultiplier (PM) (Hamamatsu Photonics R5509-72, Japan). The time-resolved PL was measured from 8 to 150 K using a time-correlated single photon counting setup. A mode-locked Ti:sapphire laser was used as the excitation source. The excitation wavelength, power, and repetition rate were 783 nm, 4 mW, and 0.8 MHz, respectively.

III. RESULTS AND DISCUSSION

A. Growth of β-$FeSi_2$ film

Epitaxial growth of β-$FeSi_2$ films on Si(111) by RDE was reported by Mahan, Thanh, Chavrier, Berbezier, Derrien, and Long,[15] but the detailed growth conditions were not described. Figure 1 shows θ-2θ XRD patterns of β-$FeSi_2$ films grown at different temperatures by RDE. The diffraction peaks of β-$FeSi_2$(440) and/or β-$FeSi_2$(404) were observed for the samples grown above 650°C, showing that the [110]- and/or [101]-oriented epitaxial β-$FeSi_2$ was formed. It is difficult to distinguish the diffraction peaks of β-$FeSi_2$(440) and β-$FeSi_2$(220) from those of β-$FeSi_2$(404) and β-$FeSi_2$(202), respectively, due to the small differences in the orthorhombic

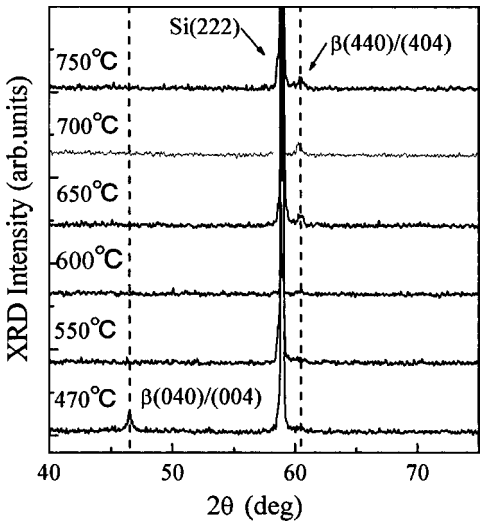

FIG. 1. θ-2θ XRD patterns of β-$FeSi_2$ films grown at different temperatures by RDE.

b and *c* of β-$FeSi_2$.[16] Two arrangements of the β-$FeSi_2$ domains, that is β-$FeSi_2$[110]/Si[111] and β-$FeSi_2$[101]/Si[111], are therefore thought to coexist in the samples.[15] Thus, the expression "[110]/[101]-oriented β-$FeSi_2$" will hereafter be used to denote the epitaxial film. At temperatures below 600°C, however, [110/101]-oriented epitaxial β-$FeSi_2$ does not form. The diffraction peak corresponding to the β-$FeSi_2$(040)/(004) was observed for the sample grown at 470°C. In order to determine the optimum growth temperature for RDE, the rms roughness of the samples grown at 650, 700, and 750°C was compared by AFM. The values were determined to be 8.8, 11.7, and 18.6 nm, respectively, and therefore the optimum growth temperature was determined to be approximately 650°C. This temperature is about 200°C higher than that for RDE of β-$FeSi_2$ on Si(001).[17,18]

Figure 2 shows θ-2θ XRD patterns of the β-$FeSi_2$ films grown by MBE at different temperatures on the template formed at 650°C by RDE. As shown in Fig. 2, the β-$FeSi_2$(220)/(202) peak dominated over the entire tempera-

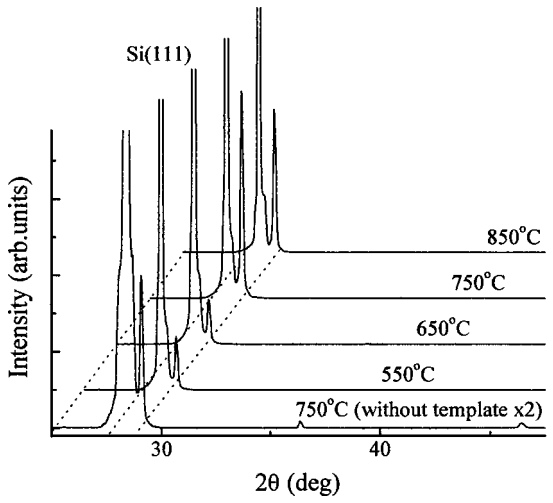

FIG. 2. θ-2θ XRD patterns of β-$FeSi_2$ films grown at different temperatures by MBE.

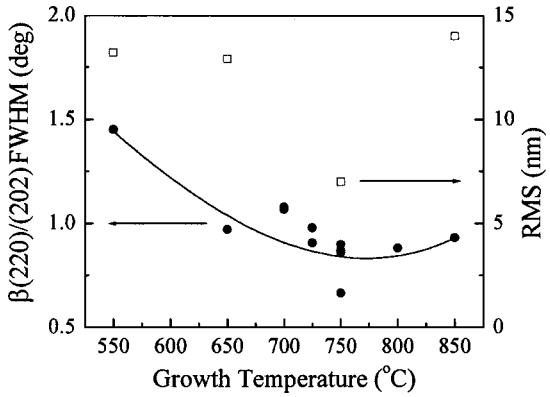

FIG. 3. Growth temperature dependence of XRD ω-scan FWHM (●) of a β-$FeSi_2$(220)/(202) peak and rms roughness value (□).

ture range. On the other hand, for the β-$FeSi_2$ film grown at 750°C without the template, the intensity of the β-$FeSi_2$(220)/(202) diffraction peak was about one-fourth of that grown at 750°C with the template. Other peaks corresponding to β-$FeSi_2$(400) and β-$FeSi_2$(040)/(004) planes were also observed at $2\theta = 36.4$ and 46.5°, respectively. The presence of these peaks indicates that it is difficult to control the crystal orientation of β-$FeSi_2$ without the template. Thus, the introduction of an epitaxial template is a very effective means of growing a [110]/[101]-oriented β-$FeSi_2$ epitaxial film by MBE. The effect of the template was also confirmed in the growth of β-$FeSi_2$ on a Si(001) substrate.[10] In order to determine the optimum MBE growth temperature, the ω scan full width at half maximum (FWHM) of the β-$FeSi_2$(220)/(202) diffraction peak intensity and the rms roughness were plotted in Fig. 3. As can be seen in Fig. 3, the FWHM initially decreases with increasing growth temperature, up to approximately 750°C. The FWHM reaches its minimum of 0.6° for the sample grown at 750°C. The growth temperature dependence of the rms roughness showed the same trend as that for FWHM. The rms roughness was at a minimum for the sample grown at 750°C. Figure 4 shows the tilted-angle SEM images of the β-$FeSi_2$ films grown at (a) 650, (b) 750, and (c) 850°C. As seen in Fig. 4, the β-$FeSi_2$ film grown at 750°C was smoother than the other two samples. These findings suggest that the optimum growth temperature of a β-$FeSi_2$ film by MBE is around 750°C.

B. Growth of Si/β-$FeSi_2$/Si structure

For fabrication of a Si/β-$FeSi_2$/Si DH, a MBE-Si overlayer was grown at the low temperature of 500°C, due to the strong islanding tendency of Si observed when grown at higher temperatures, such as 750°C. Figure 5(a) shows the tilted-angle SEM image of sample A, obtained by annealing the Si(300 nm)/β-$FeSi_2$/Si structure at 900°C for 14 h. The white parts correspond to β-$FeSi_2$. As can be seen, the β-$FeSi_2$ islands moved up to the surface, showing that a β-$FeSi_2$ continuous film cannot be embedded in Si under these growth conditions. The same result was obtained for sample B, which was formed by annealing the same Si(300 nm)/β-$FeSi_2$/Si structure at 800°C for 14 h. These results suggested that a 300-nm-thick Si overlayer was not sufficient to

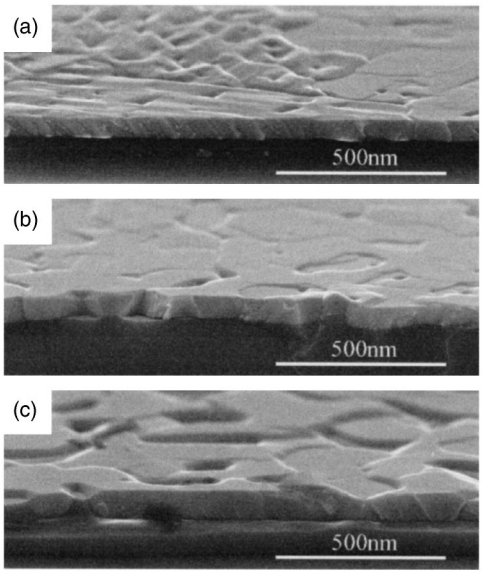

FIG. 4. Tilted-angle cross-sectional SEM images of β-$FeSi_2$ films grown by MBE at (a) 650, (b) 750, and (c) 850°C.

prevent the aggregation of a 90-nm-thick β-$FeSi_2$ film. Thus, the thickness of the Si overlayer increased from 300 to 900 nm in samples D and E. Figure 5(b) shows the SEM cross section of sample D, prepared by annealing the Si(900 nm)/β-$FeSi_2$/Si structure at 900°C for 14 h. The β-$FeSi_2$ aggregated in the Si matrix. RDE-grown β-$FeSi_2$ films are known to exhibit a strong tendency to form islands,[9] in particular during high-temperature annealing.[11] The aggregation of β-$FeSi_2$ was thought to occur in order to decrease the β-$FeSi_2$/Si interface energy due to the lattice mismatch between the two materials with decreasing contact area. High-temperature annealing is expected to result in intense PL, as later described; therefore, the annealing tem-

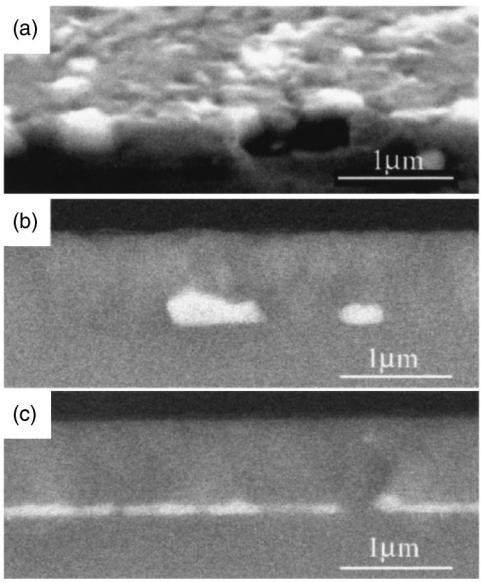

FIG. 5. Tilted-angle SEM images of the Si/β-$FeSi_2$/Si structure of (a) sample A, obtained after annealing at 900°C. The thickness of the Si overlayer is 300 nm. (b) and (c) are cross-sectional SEM images of samples D and E, obtained after annealing 900°C, 800°C, respectively. The thickness of the Si overlayer is 900 nm.

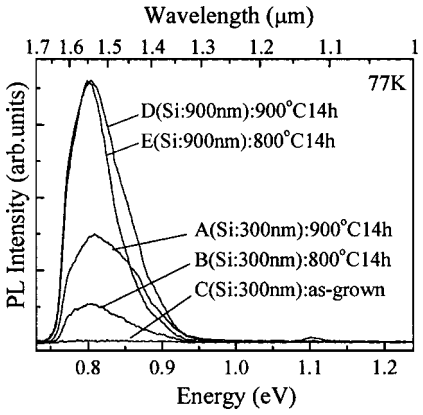

FIG. 6. PL spectra measured at 77 K for samples A–F.

perature was lowered from 900 to 800 °C. As shown in Fig. 5(c), the β-$FeSi_2$ continuous film was successfully embedded in a Si matrix in sample E. These results demonstrated that both the thickness of the Si overlayer and the annealing temperature are key parameters in forming a Si/β-$FeSi_2$/Si DH.

C. Photoluminescence

Figure 6 shows the PL spectra measured at 77 K. PL was not obtained from the as-grown samples of C and F. This is probably because the Si overlayer grown at 500 °C contains numerous defects, and thus photoexcited carriers nonradiatively recombine via the defect levels. In contrast, PL was obtained from the annealed samples. The PL intensity was observed to increase with increasing thickness of the Si overlayer. This phenomenon is attributed to the increase in photoexcited carriers generated in the Si overlayer. However, all spectra obtained for samples A, B, and D, which contain the aggregated β-$FeSi_2$ particles, were broader than the spectra for sample E. Transmission electron microscopy (TEM) observation revealed that the large-sized β-$FeSi_2$ particles embedded in Si induced dislocations in the surrounding Si.[19] Stressed Si has been reported to introduce dislocations as well as exhibit characteristic *D*-line emissions.[20–22] The origin of these broad PL spectra are therefore thought to be the dislocations. Although we obtained 1.55 μm PL from the Si/β-$FeSi_2$/Si DH as shown in Fig. 6, a simple cw PL measurement alone cannot distinguish the luminescence of β-$FeSi_2$ from a *D*1 line because the *D*1 line corresponds to the same emission line for β-$FeSi_2$ at low temperatures. A detailed discussion on the origin and nature of the luminescence from β-$FeSi_2$ precipitates in Si has been recently reported by Grimaldi *et al.* and Martinelli *et al.*[23,24] We think that time-resolved PL measurement, compared to cw PL measurements, is one of the most powerful methods of investigating the intrinsic optical properties of β-$FeSi_2$. This is because a band-to-band direct transition is generally characterized by a short decay time. There have been only four reports discussing the decay time of PL line of β-$FeSi_2$,[25–28] and there is no report on a PL decay time of β-$FeSi_2$ grown by RDE and by MBE. Chu *et al.* reported a fast PL-decay time of subnanosecond in β-$FeSi_2$ films formed by the magnetron-sputtering technique.[28] However, we cannot rule out the possibility that the measured PL-decay time was

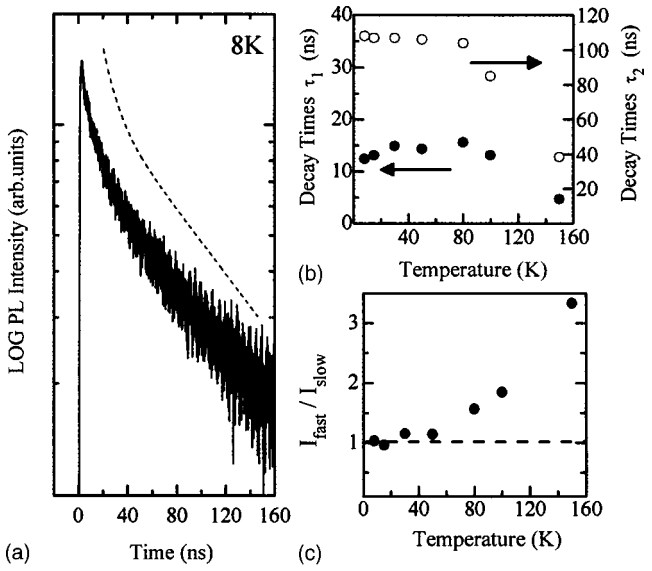

FIG. 7. (a) Time-resolved PL decay curve of the 1.55 μm emission at 8 K. (b) The observed PL decay times vs temperature obtained from the decay curves. (c) Temperature dependence of the PL intensity ratio of the fast I_{fast} to the slow component I_{slow}.

dominated by nonradiative recombination process because the evaluation of the temperature dependence of the PL-decay time was lacking.

Figure 7(a) shows the PL decay curve of the 1.55 μm peak in sample E measured at 8 K. The time resolution of the system was about 1 ns. This decay curve could not be fitted to one exponential decay curve. In contrast, the decay curve obtained from the Si/β-$FeSi_2$ particles/Si(001) structure grown by MBE was well-described by a single-decay time.[29] In order to estimate the decay time, the decay curve shown in Fig. 7(a) was fitted using Eq. (1), which is based on the assumption that it was composed of the sum of two exponentials, as discussed by Schuller *et al.*[26,27]

$$I(t) = I_1 \exp\left(-\frac{t}{\tau_1}\right) + I_2 \exp\left(-\frac{t}{\tau_2}\right). \quad (1)$$

Here, I_1 and I_2 are the PL intensities of the components with decay times τ_1 and τ_2, respectively. The curve shifted upwards, as seen in Fig. 7. Good agreement was obtained with the experimental curve when τ_1 and τ_2 were 12 ns and 104 ns, respectively. This finding indicates that the 1.55 μm PL originated from two sources. Figure 7(b) shows the obtained PL decay time vs. temperature plot. The short decay time τ_1 was found to be almost the same as the decay time obtained in the Si/β-$FeSi_2$ particles/Si(001) structure (τ =5 ns at 8 K).[29] This short decay time is about three orders of magnitude smaller than that previously reported in IBS.[25,26] The short-decay time increased with temperature at low temperatures and then decreased above a critical temperature (~50 K). This decay-time behavior was reported to be typical for excitons,[30,31] indicating that the nonradiative recombination process was negligible at the lowest temperature measured. Therefore, this decay was thought to be attributable to the recombination in β-$FeSi_2$. The β-$FeSi_2$ particles embedded in Si by MBE at 500 °C were found to be

under tensile strain in the α-axis direction[6] and thus we suppose that they have a direct band gap nature. We therefore speculate that the β-$FeSi_2$ film is also strained as in the case of the β-$FeSi_2$ particles. Unfortunately, we have no definite information to discuss strain and thus further study will be needed. On the other hand, the long-decay time τ_2 is thought to be due to the $D1$ luminescence, because the $D1$ line is another possible origin of the 1.55 μm PL. In addition, the long-decay time obtained was comparable with the reported $D1$-decay time.[32] The origin of the short and long decay times are therefore thought to be due to the recombination in β-$FeSi_2$ and the defects in the Si, respectively. Figure 6(c) shows the temperature dependence of the PL intensity ratio of the fast I_{fast} to the slow I_{slow} component. The ratio I_{fast}/I_{slow} was almost one at the low temperature, but increased as the temperature increased. This increase was thought to be because the $D1$ line was more rapidly quenched, indicating that PL from β-$FeSi_2$ dominates at higher temperatures.

IV. SUMMARY

Highly-oriented β-$FeSi_2$ continuous films and Si/β-$FeSi_2$/Si DH were grown on Si (111) substrates by RDE and by MBE. The [110]/[101]-oriented β-$FeSi_2$ continuous films with smooth surfaces were obtained by MBE at 750 °C using a β-$FeSi_2$ epitaxial template formed by RDE at 650 °C. In order to prevent aggregation of β-$FeSi_2$ and to form the Si/β-$FeSi_2$/Si DH, both the thickness of the Si overlayer and the annealing temperature were important. Strong 1.55 μm PL was obtained from the DH. Time-resolved PL measurements showed that the 1.55 μm PL originated from two sources; recombination in β-$FeSi_2$ and the dislocation-related $D1$ line emission.

ACKNOWLEDGMENTS

This work was supported in part by Grants-in-Aid for Scientific Research (B)(12450137 and 12555084) from the Ministry of Education, Culture, Sports, Science and Technology (MEXT) of Japan, the TARA project at the University of Tsukuba, and the Industrial Technology Research Grant Program in 2002 from the New Energy and Industrial Technology Development Organization (NEDO) of Japan. The authors express their sincere thanks to Dr. T. Koyano (Cryogenics Center at the University of Tsukuba) for his help in SEM observation.

[1] M. C. Bost, and J. E. Mahan, J. Appl. Phys. **58**, 2696 (1985).
[2] D. Leong, M. Harry, K. J. Reeson, and K. P. Homewood, Nature (London) **387**, 686 (1997).
[3] M. A. Lourenco, T. M. Butler, A. K. Kewell, R. M. Gwilliam, K. J. Kirkby, and K. P. Homewood, Jpn. J. Appl. Phys., Part 1 **40**, 4041 (2001).
[4] L. Martinelli, E. Grilli, M. Guzzi, and M. G. Grimaldi, Appl. Phys. Lett. **83**, 794 (2003).
[5] T. Suemasu, Y. Negishi, K. Takakura, and F. Hasegawa, Jpn. J. Appl. Phys., Part 2 **39**, L1013 (2000).
[6] T. Suemasu, Y. Negishi, K. Takakura, F. Hasegawa, and T. Chikyow, Appl. Phys. Lett. **79**, 1804 (2001).
[7] S. Chu, T. Hirohada, H. Kan, and T. Hiruma, Jpn. J. Appl. Phys., Part 2 **43**, L154 (2004).
[8] T. D. Hunt, B. J. Sealy, K. J. Reeson, R. M. Gwilliam, K. P. Homewood, R. J. Wilson, C. D. Meekison, and G. R. Booker, Nucl. Instrum. Methods Phys. Res. B **74**, 60 (1993).
[9] K. M. Geib, J. E. Mahan, R. G. Long, and M. Nathan, J. Appl. Phys. **70**, 1730 (1991).
[10] N. Hiroi, T. Suemasu, K. Takakura, N. Seki, and F. Hasegawa, Jpn. J. Appl. Phys., Part 2 **40**, L1008 (2001).
[11] T. Suemasu, M. Tanaka, T. Fujii, S. Hashimoto, Y. Kumagai, and F. Hasegawa, Jpn. J. Appl. Phys., Part 2 **36**, L1225 (1997).
[12] T. Suemasu, Y. Iikura, T. Fujii, K. Takakura, N. Hiroi, and F. Hasegawa, Jpn. J. Appl. Phys., Part 2 **38**, L620 (1999).
[13] C. Lin, L. Wang, X. Chen, L.-F. Chen, and L.-M. Wang, Jpn. J. Appl. Phys., Part 1 **37**, 622 (1998).
[14] T. Koga, H. Tatsuoka, and H. Kuwabara, Appl. Surf. Sci. **169/170**, 310 (2001).
[15] J. E. Mahan, V. Le. Thanh, J. Chevrier, I. Berbezier, J. Derrien, and R. G. Long, J. Appl. Phys. **74**, 1747 (1993).
[16] Y. Dusausoy, J. Protas, R. Wandji, and B. Roques, Acta Crystallogr., Sect. B: Struct. Crystallogr. Cryst. Chem. **27**, 1209 (1971).
[17] J. E. Mahan, K. M. Geib, G. Y. Robinson, R. G. Long, X. Yan, G. Bai, M. A. Nicolet, and M. Nathan, Appl. Phys. Lett. **56**, 2126 (1990).
[18] M. Tanaka, Y. Kumagai, T. Suemasu, and F. Hasegawa, Jpn. J. Appl. Phys., Part 1 **36**, 3620 (1997).
[19] T. Suemasu, T. Fujii, M. Tanaka, K. Takakura, Y. Iikura, and F. Hasegawa, J. Lumin. **80**, 473 (1999).
[20] D. A. Drozdov, A. A. Patrin, and V. D. Tkachev, Sov. Phys. JETP **23**, 597 (1976).
[21] B. Suezawa, Y. Sasaki, and K. Sumio, Phys. Status Solidi A **79**, 173 (1983).
[22] R. Sauer, J. Weber, J. Stolz, E. Weber, K. Kusters, and H. Alexander, Appl. Phys. A: Solids Surf. **36**, 1 (1985).
[23] Grimaldi *et al.*, Phys. Rev. B **66**, 085319 (2002).
[24] Martinelli *et al.*, Phys. Rev. B **66**, 085320 (2002).
[25] C. Spinella, S. Coffa, C. Bongiorno, S. Pannitteri, and M. G. Grimaldi, Appl. Phys. Lett. **76**, 173 (2000).
[26] B. Schuller, R. Carius, S. Lenk, and S. Mantl, Microelectron. Eng. **60**, 205 (2002).
[27] B. Schuller, R. Carius, and S. Mantl, J. Appl. Phys. **94**, 207 (2003).
[28] S. Chu, T. Hirohada, M. Kuwabara, H. Kan, and T. Hiruma, Jpn. J. Appl. Phys., Part 2 **43**, L127 (2004).
[29] T. Suemasu, M. Takauji, C. Li, Y. Ozawa, M. Ichida, and F. Hasegawa, Jpn. J. Appl. Phys., Part 2 **43**, L930 (2004).
[30] W. Yang, R. R. Lowe-Webb, H. Lee, and P. C. Sercel, Phys. Rev. B **56**, 13314 (1997).
[31] Y. Terai, S. Kuroda, K. Takita, T. Okuno, and Y. Masumoto, Appl. Phys. Lett. **73**, 3757 (1998).
[32] S. Fukatsu, Y. Mera, M. Inoue, K. Maeda, H. Akiyama, and H. Sakaki, Appl. Phys. Lett. **68**, 1889 (1996).